

# Ionogels, New Materials Arising from the Confinement of Ionic Liquids within Silica-Derived Networks

Marie-Alexandra Néouze,<sup>†</sup> Jean Le Bideau,<sup>†</sup> Philippe Gaveau,<sup>‡</sup> Séverine Bellayer,<sup>†</sup> and André Vioux<sup>\*,†</sup>

*Chimie Moléculaire et Organisation du Solide (UMR CNRS 5637) and Laboratoire de Physicochimie de la Matière Condensée (UMR CNRS 5617), Institut Charles Gerhardt, Université Montpellier 2, 34095 Montpellier, France*

Received March 19, 2006. Revised Manuscript Received June 18, 2006

A simple nonaqueous sol–gel processing led to ionogels, resulting in the confinement of an ionic liquid within a silica-like network. In the case of a non-water-soluble ionic liquid, ionogels were made stable toward water immersion by the presence of hydrophobic methyl groups in the solid network. A set of ionogels with different ionic liquid content was studied by DSC and <sup>1</sup>H NMR spectroscopy. The nanometric level of the confinement of the ionic liquid turned out to significantly modify the phase transitions, while still allowing some molecular mobility. Moreover, ionogels were found to keep the high conducting performances of the ionic liquid.

## Introduction

Room-temperature ionic liquids are generally salts of an organic cation (ammonium, phosphonium, imidazolium, pyridinium, etc.). Their chemical and physical properties may be quite varied, as they can be tuned by choosing a specific combination of cation and anion among numerous possibilities. Some ionic liquids, as imidazolium salts, are currently widely used as alternative solvents, because of their negligible vapor pressure, thermal stability, and nonflammability. Typically, they attract much attention in organic synthesis, especially in organometallic catalysis processes, in relation to their ability to be recovered and recycled.<sup>1</sup> However, these ionic liquids have been known for a long time by electrochemists for their high ionic conductivity and their wide electrochemical potential window<sup>2</sup> and have recently been studied as electrolytes in fuel cells, solar cells, and lithium batteries.<sup>3–7</sup>

For such applications as electrolyte membranes and catalysis processing, there is a need for immobilizing ionic liquids on solid supports or within a solid matrix.<sup>8–10</sup> It is

worth noting that systems involving discrete anchoring of ionic groups (e.g., imidazolium groups) onto solids may be of interest, especially for catalysis applications, but they cannot be regarded as supported ionic liquids as long as no liquid phase is concerned.<sup>8,11,12</sup> Actually, there are mainly two classes of systems for immobilizing ionic liquids depending on whether the solid network is organic (polymer) or inorganic (oxide). Moreover, within each class, two ways of preparation may be distinguished, depending on whether the solid network is achieved in situ or not: (i) by carrying out either polymerization<sup>13,14</sup> or sol–gel<sup>15–17</sup> in the ionic liquid, or (ii) by swelling of polymers<sup>18,19</sup> or impregnation of oxide particles.<sup>20–23</sup>

The basic idea that is developed in the sol–gel method is to confine the ionic liquid within an oxide matrix through a one-step process. A gel (usually aquogel or alcogel) is defined as a solid interconnected network spreading through-

\* Corresponding author. E-mail: vioux@univ-montp2.fr.

<sup>†</sup> Chimie Moléculaire et Organisation du Solide, Université Montpellier.

<sup>‡</sup> Laboratoire de Physicochimie de la Matière Condensée, Université Montpellier.

- (1) Wasserscheid, P.; Welton, T. *Ionic Liquids in Synthesis*; Wiley–VCH Verlag: Weinheim, Germany, 2003.
- (2) Ohno, H., Ed. *Electrochemical Aspects of Ionic Liquids*; John Wiley & Sons: Hoboken, NJ, 2005.
- (3) Xu, W.; Angell, C. A. *Science* **2003**, *302*, 422–425.
- (4) Noda, A.; Susan, M. A. B. H.; Kudo, K.; Mitsushima, S.; Hayamizu, K.; Watanabe, M. *J. Phys. Chem. B* **2003**, *107*, 4024–4033.
- (5) Wang, P.; Zakeeruddin, S. M.; Humphry-Baker, R.; Graetzel, M. *Chem. Mater.* **2004**, *16*, 2694–2696.
- (6) Seki, S.; Kobayashi, Y.; Miyashiro, H.; Ohno, Y.; Usami, A.; Mita, Y.; Kihira, N.; Watanabe, M.; Terada, N. *J. Phys. Chem. B* **2006**, *110*, 10228–10230.
- (7) Kuang, D.; Ito, S.; Wenger, B.; Klein, C.; Moser Jacques, E.; Humphry-Baker, R.; Zakeeruddin Shaik, M.; Graetzel, M. *J. Am. Chem. Soc.* **2006**, *128*, 4146–4154.
- (8) Valkenberg, M. H.; de Castro, C.; Hölderich, W. F. *Green Chem.* **2002**, *4*, 88.

- (9) Mehnert, C. P. *Chem.–Eur. J.* **2005**, *11*, 50.
- (10) Rissager, A.; Fehrmann, R.; Haumann, M.; Wasserscheid, P. *Eur. J. Inorg. Chem.* **2006**, 695.
- (11) Fraga-Dubreuil, J.; Bazureau, J. P. *Tetrahedron Lett.* **2001**, *42*, 6097.
- (12) Gadenne, B.; Hesemann, P.; Moreau, J. J. E. *Chem. Commun.* **2004**, 1768.
- (13) Watanabe, M. *Polym. Prepr.* **2004**, *45*, 303.
- (14) Klingshirn, M. A.; Spear, S. K.; Subramanian, R.; Holbrey, J. D.; Huddleston, J. G.; Rogers, R. D. *Chem. Mater.* **2004**, *16*, 3091.
- (15) Li, D.; Shi, F.; Guo, S.; Deng, Y. *Tetrahedron Lett.* **2004**, *45*, 265.
- (16) Néouze, M.-A.; Le Bideau, J.; Leroux, F.; Vioux, A. *Chem. Commun.* **2005**, 1082.
- (17) Liu, Y.; Wang, M.; Li, J.; Li, Z.; He, P.; Liu, H.; Li, J. *Chem. Commun.* **2005**, 1778.
- (18) Carlin, R. T.; Fuller, J. *Chem. Commun.* **1997**, 7, 1345.
- (19) Fuller, J.; Breda, A. C.; Carlin, R. T. *J. Electrochem. Soc.* **1998**, *459*, 29.
- (20) Mehnert, C. P.; Mozeleski, E. J.; Cook, R. A. *Chem. Commun.* **2002**, 3010.
- (21) Mehnert, C. P.; Cook, R. A. (ExxonMobil Co.) PCT Int. Appl. WO, 2002.
- (22) Mehnert, C. P.; Cook, R. A.; Dispenziere, N. C.; Afeworki, M. J. *Am. Chem. Soc.* **2002**, *124*, 12932.
- (23) Wang, P.; Zakeeruddin, S. M.; Comte, P.; Exnar, I.; Graetzel, M. J. *Am. Chem. Soc.* **2003**, *125*, 1166.

out a liquid phase. In classical sol–gel processing, the liquid phase is removed, the targeted material being the porous (oxide) solid obtained after drying (xerogel or aerogel). However, the use of liquids without measurable vapor pressure, such as ionic liquids, permits us to regard the gel itself, a stable solid–liquid system called an ionogel, as a material. It is worth stressing that the objective is quite different from using ionic liquids as templates, generally in aqueous sol–gel processes, even though it is of interest to note that ionic liquids are able to induce porosity in silica matrixes.<sup>24–27</sup>

Recently, we reported the straightforward one-pot synthesis of monolith ionogels, cast as pellets or rods, which were shown to be endowed with both the transparency and mechanical properties of silica and the conductivity performances of ionic liquids.<sup>16,28</sup> The present paper focuses on the synthesis and characterization of a set of ionogels derived from [BMI][TFSI] (1-butyl-3-methylimidazolium bis(trifluoromethylsulfonyl)amide). We report herein (i) the influence of the nature of the matrix (silica or organically modified silica) upon the stability of ionogels toward solvents (including water) and heating; (ii) the influence of ionic liquid contents upon the texture of silica networks; and (iii) first insights into the effect of the confinement of the ionic liquid (the effect that depends on the liquid-to-solid ratio) on phase transitions, molecular mobility (on the basis of DSC and <sup>1</sup>H NMR), and ionic conduction.

## Experimental Section

**Material Synthesis.** 1-Butyl-3-methylimidazolium bis(trifluoromethylsulfonyl)amide [BMI][TFSI] was synthesized as a colorless transparent liquid according to the literature:<sup>29</sup> 1-methylimidazole was reacted with a slight excess of 1-bromobutane in a round-bottom flask and left refluxing for 3 h to produce 1-butyl-3-methylimidazolium bromide [BMI][Br]. The corresponding [TFSI] salt was then prepared by metathesis of [BMI][Br] in water with sodium bis(trifluoromethylsulfonyl)amide. Ionogels were prepared as previously published by Vioux et al.<sup>16,28</sup> using a non-hydrolytic sol–gel route: tetramethoxysilane (TMOS; purchased from Fluka), or a mixture of TMOS and methyltrimethoxysilane (MTMS; purchased from Alfa Aesar), was added to a solution of formic acid (FA) in [BMI][TFSI] (molar ratio FA/TMOS or FA/(TMOS+MTMS) = 7.8/1). After a short stirring, gelation occurred within 1 h for a TMOS ionogel, or within 36 h for a TMOS/MTMS ionogel. Aging in a room-temperature bath with exposure to ultrasound (12 W power, 2 s pulse) was carried out overnight.

**Material Characterization.** Thermogravimetric analyses (TGA) were carried out with a Netzsch STA 409 TGA analyzer, and data were evaluated with Proteus Thermal Analysis software, version 4.3.1. All samples were run in aluminum pans at a heating rate of 2 K min<sup>-1</sup> from 295 to 873 K, under a 50 cm<sup>3</sup> min<sup>-1</sup> air flow. The

**Table 1. Ionogels: Compositions, Surface Areas, and Pore Volume**

precursor	ionic liquid/precursor (x mol/mol)	surface area (m <sup>2</sup> g <sup>-1</sup> )	pore volume (cm <sup>3</sup> g <sup>-1</sup> )
TMOS	0.25	850	1.1
TMOS	0.5	780	1.5
TMOS	1	830	3.2
TMOS/MTMS (1/1)	0.5	780	0.6
TMOS/MTMS (1/1)	1	870	0.8

experiments were carried out on samples ground into powder (and on pure ionic liquid). Measurements of phase-transition temperatures were done with a Netzsch differential scanning calorimeter, model 204 F1 Phoenix, and the data were evaluated using Netzsch Proteus Thermal Analysis software version 4.8.1. Samples of 10–15 mg were placed in a hermetically sealed aluminum pan; an empty pan was used as a reference. Pans were exposed to a N<sub>2</sub> flow atmosphere. Measurements for the melting, crystallization, and glass-transition temperatures were determined by cooling the sample to –120 °C at a rate of 50 °C/min, followed by heating from –120 to 150 °C at a rate of 10 °C/min. The glass transition was determined at the midpoint of a heat-capacity change, whereas the melting and crystallization temperatures were determined at the onset of the transition.

A Micrometrics ASAP 2010 analyzer (accelerated surface area and porosimetry system) was used to measure the surface area and porosity of ionogels using dinitrogen at 77 K as the standard adsorptive gas. Ionogels (800–1000 mg) ground into powder were introduced into the experimental tubes. Samples were left for 12 h under a vacuum at 120 °C before the experiment was performed.

<sup>1</sup>H liquid-state NMR spectra were obtained using SiMe<sub>4</sub> as reference on a Bruker 200. <sup>1</sup>H solid-state NMR was performed on ground samples on a Bruker ASX400 using a standard 4 mm CPMAS probe. For the temperature experiments, we used the following procedure: cooling from room temperature to 170 K (around 30 min) and waiting 1 h 30 min for stabilization. Next, raise by 10 K steps and wait 15 min before each measurement (30 min for a 20 K step).

Alternating-current conductivity measurements were carried out with platinum electrodes on a Novocontrol apparatus, with a frequency range from 1 MHz to 10 Hz, cycling from 520 to 180 K and return.

## Results

**Sol–Gel Processing.** For this study, we chose to use [BMI][TFSI] (1-butyl-3-methylimidazolium bis(trifluoromethylsulfonyl)amide), as this ionic liquid combines low viscosity, good ionic conductivity, and immiscibility with water and solvents of low polarity such as alkanes, ethers, etc.<sup>29</sup> We used the mild sol–gel method provided by the reaction of formic acid with alkoxy silanes, typically tetramethoxysilane (TMOS) or a mixture of TMOS and methyltrimethoxysilane (MTMS). This reaction reported by Sharp et al.<sup>30</sup> involves the formation of silicon formate species with the release of alcohol; the subsequent esterification reaction likely provides water, which subsequently causes hydrolytic condensations, even though nonhydrolytic condensations are not precluded. Anyway, methylformate is mainly formed as byproduct.<sup>30</sup> Typical TMOS/formic acid/[BMI][TFSI] molar ratios used were *x*/1/7.8, with *x* ranging from 0.25 to 1 (Table 1). Gelation occurred within 90 min. Crack-free transparent pellets were obtained, the weight of which became constant

(24) Dai, S.; Ju, Y. H.; Gao, H. J.; Lin, J. S.; Pennycook, S. J.; Barnes, C. E. *Chem. Commun.* **2000**, 3, 243.

(25) Antonietti, M.; Kuang, D.; Smarsly, B.; Zhou, Y. *Angew. Chem., Int. Ed.* **2004**, 43, 4988.

(26) Liu, Y.; Wang, M.; Li, Z.; Liu, H.; He, P.; Li, J. *Langmuir* **2005**, 21, 1618.

(27) Zhou, Y. *Curr. Nanosci.* **2005**, 1, 35.

(28) Néouze, M.-A.; Le Bideau, J.; Vioux, A. *Prog. Solid State Chem.* **2005**, 33, 217–222.

(29) Bonhôte, P.; Dias, A.-P.; Papageorgiou, N.; Kalyanasundaram, K.; Graetzel, M. *Inorg. Chem.* **1996**, 35, 1168.

(30) Sharp, K. G. J. *Sol–Gel Sci. Technol.* **1994**, 2, 35.

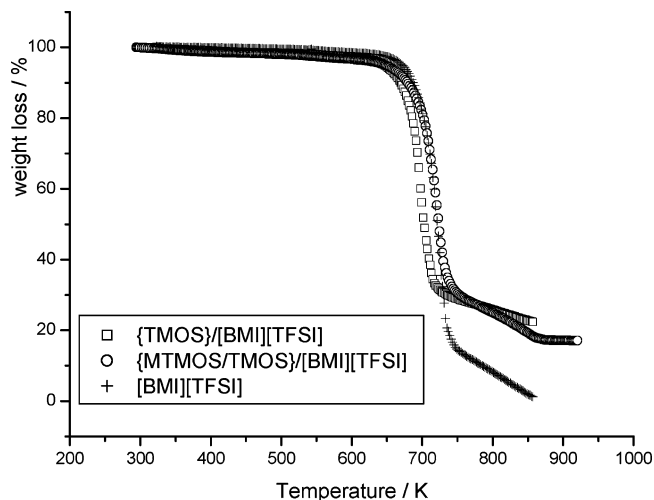


**Figure 1.** TGA traces of the ionic liquid ([BMI][TFSI]), a silica-based ionogel ( $x = 0.5$ ), and a methyl-modified ionogel (TMOS/MTMOS 1/1;  $x = 0.5$ ).

after aging for a few days at room temperature or for a few hours upon exposure to ultrasound. Quantitative  $^{29}\text{Si}$  solid-state NMR spectroscopy indicated a condensation extent of about 90%.

**Stability toward Solvents.** An important question with respect to many applications is whether ionogels can be used in the presence of water or organic solvents, or whether the ionic liquid is removed from the host matrix. Actually, ionogels were found to be quite stable when immersed into an organic solvent as long as the ionic liquid was not soluble in this solvent (e.g., in toluene). Conversely, the ionic liquid could be extracted from the gel by polar solvents such as acetonitrile, dichloromethane, or ethanol, which dissolved the ionic liquid.

The case of water was specific. Although [BMI][TFSI] was nonsoluble in water, it was easily removed from the gels when immersed in water. However, we showed that the incorporation of methyl groups (by adding some amount of MTMS) made the ionogels completely stable toward water.

**Thermal Stability.** As expected, the ionogels exhibited the same stability at high temperature as the ionic liquids alone; in both cases, thermogravimetric analyses carried out at a slow heating rate ( $2 \text{ K min}^{-1}$ ) under an ambient atmosphere indicated the total degradation of the ionic liquid at ca.  $370 \text{ }^\circ\text{C}$ . It is noteworthy that the incorporation of a large amount of methyl groups, by using a TMOS/MTMS molar ratio as high as 50/50, had no significant effect on the thermal stability (Figure 1).

**Characterization of Silica Networks.** The complete extraction of ionic liquid by acetonitrile by means of Soxhlet was checked by proton NMR and IR spectroscopy; the absence of any residual ionic liquid gave evidence of the interconnected open porosity of ionogels. To characterize the texture of the inorganic skeletons, we washed out the ionic liquid from a set of ionogel samples synthesized from TMOS. The  $\text{N}_2$  sorption isotherms of the silica skeletons were found to be typical of a mesoporous solids (Figure 2), giving evidence of the nanometer scale of confinement of the ionic liquid within the silica matrix (even though some slight shrinkage of the pores during the extraction of the ionic

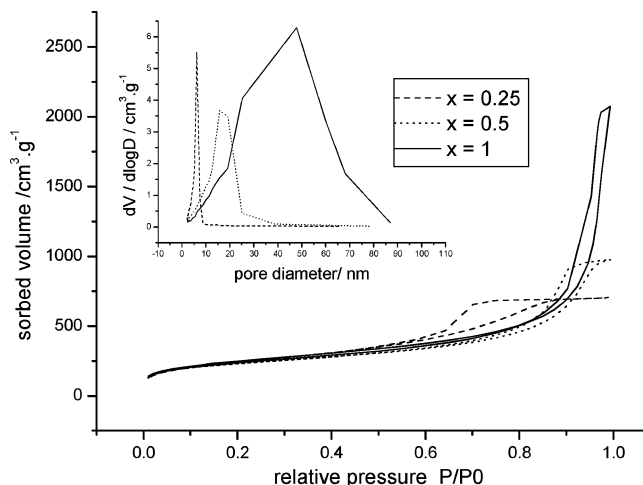


**Figure 2.**  $\text{N}_2$  sorption measurements: (a) isotherms for silica-based gels with different contents of ionic liquid [BMI][TFSI]; (b) insert, pore diameter distributions (calculated from the desorption branch of the isotherm using the BJH method).

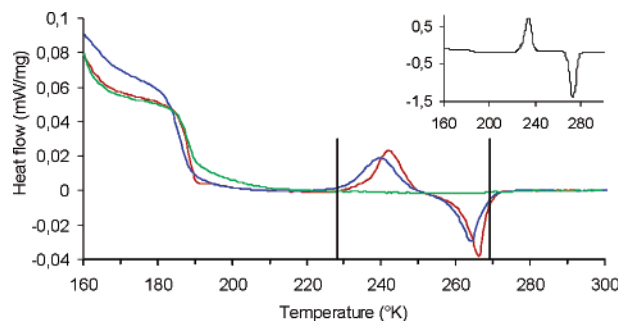


**Figure 3.** DSC traces of two silica-based ionogels ( $x = 0.5$ , green;  $x = 1$ , red) and one methyl-modified ionogel (TMOS/MTMOS 1/1;  $x = 1$ , blue). Insert: pristine ionic liquid ([BMI][TFSI]).

liquid cannot be precluded, especially in the less-cross-linked samples arising from mixed TMOS/MTMS compositions). The calculated specific surface areas and pore volumes (Table 1) were found to be consistent with a high open porosity. The diameters of pores and their dispersion turned out to significantly increase as the ionic liquid-to-silica molar ratio  $x$  increased as long as MTMS was not used (Figure 2b).

**Differential Scanning Calorimetry (DSC).** Some insights into the effect of confinement were given by carrying out DSC on ionogels with different contents of ionic liquid. As expected from the literature,<sup>31</sup> the DSC of the pristine ionic liquid exhibited, upon heating after a fast cooling ( $30 \text{ K min}^{-1}$ ), a glass-transition temperature ( $T_g$ ) at  $186 \text{ K}$  (the compound passed from the glass state to a “subcooled liquid” phase), an exothermic cold crystallization ( $T_{cc}$ ) at  $228 \text{ K}$ , and a subsequent endothermic melting ( $T_m$ ) at  $269 \text{ K}$  (all temperatures were determined as the onset of the transition, except the glass transition, which was determined as the midpoint of a heat-capacity change). In ionogels, confinement of the ionic liquid had a dramatic effect on DSC thermograms (Figure 3). Although the glass transition was observed in all cases (whatever  $x$  was), some occurrence of crystallization and melting was observed for  $x = 1$ , but not for  $x = 0.25$  and  $0.50$  (in either pure silica ionogel or methyl-modified

(31) Fredlake, C. P.; Crosthwaite, J. M.; Hert, D. G.; Aki, S. N. V. K.; Brennecke, J. F. *J. Chem. Eng. Data* **2004**, *49*, 954.

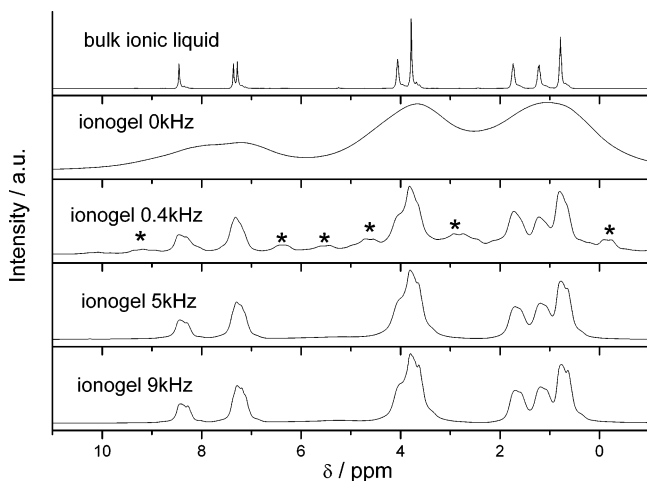


**Figure 4.** Room-temperature  $^1\text{H}$  NMR spectra of the pristine ionic liquid ([BMI][TFSI]) and a silica-based ionogel ( $x = 0.5$ ) at different spinning rates (asterisks indicate spinning sidebands).

ionogel). Moreover, for ionogels with  $x = 1$ , the temperatures of the first-order phase transition (melting) were clearly shifted to a lower value. Such a shift of the phase-transition peaks (also observed when silica walls were modified by methyl groups) has been reported for confined fluids.<sup>32</sup>

**$^1\text{H}$  NMR Spectroscopy.** The observation of proton NMR signals without spinning was quite unexpected. The full width at half-maximum (fwhm) was about 1 ppm at 400 MHz. Actually, a spinning rate as low as 0.4 kHz was enough to recover good resolution (Figure 4; stars indicate spinning sidebands). This indicated that chemical shift anisotropy and dipolar interactions were averaged in the confined ionic liquid, in agreement with a quasi-liquid behavior. However, instrumental resolution for proton resonance was not fully recovered at 0.4, 5, and 9 kHz spinning rates.

Recording the spectra at lower temperatures (Figure 5) permitted us to estimate the range of temperatures below which the resolution was lost, both in the pristine ionic liquid (Figure 5a) and in silica-based and methyl-modified ionogels ( $x = 0.5$ ; panels b and c in Figure 5). This temperature could be related to the glass transition, even though it was found to be about 30–70 K above the value arising from DSC. This discrepancy from the DSC observation could be explained allowing for the different cooling procedures; moreover, it is worth noting that, as a matter of fact, NMR spectroscopy is sensitive to phenomena featuring higher frequencies than DSC. However, on the basis of NMR, the glass-transition temperatures in ionogels were observed significantly below that of the pristine ionic liquid: about 20–30 K lower for the silica-based ionogel, and even 30–40 K lower for the methyl-modified ionogel.

**Ionic Conductivity.** The ionic conductivity of ionogels in the temperature range from 170 to 500 K was determined using the complex impedance spectroscopy carried out on an impedance analyzer from 10 Hz to 1 MHz; the conductivity  $\sigma$  was determined from the almost-frequency-independent plateau ( $\log(\sigma)$  vs  $\log(\nu)$  plot; Figure 6) The conducting behavior of ionogels gave new evidence of their interconnected porosity.

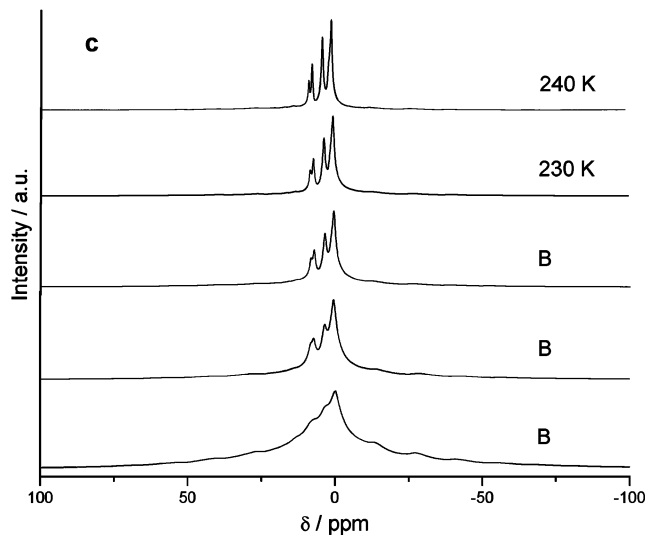
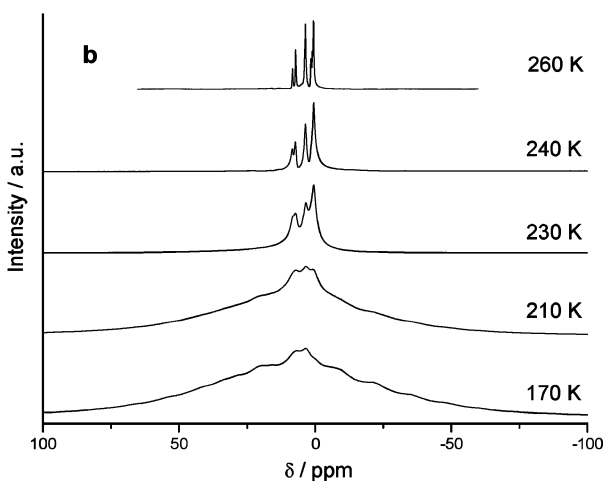
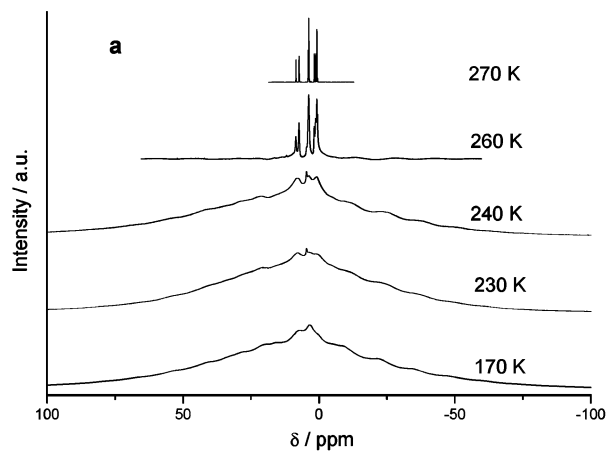


**Figure 5.** Low-temperature  $^1\text{H}$  NMR spectra (around  $T_g$ ) of (a) the pristine ionic liquid ([BMI][TFSI]), (b) a silica-based ionogel ( $x = 0.5$ ), and (c) a methyl-modified ionogel (TMOS/MTMOS 1/1;  $x = 0.5$ ).

The ionogels showed a conductivity on the same order of magnitude as the pristine ionic liquid ( $\sigma$  vs temperature plot; Figure 7). Typically, for  $x = 0.5$ , the conductivity of the ionogel near 440 K was roughly half that of the ionic liquid. The Arrhenius plots  $\log(\sigma T)$  vs  $(1 \times 10^3)/T$  (Figure 8) led to a set of curves that gradually moved apart from that of the pristine ionic liquid as the relative amount of confined ionic liquid decreased (from  $x = 1$  to  $x = 0.25$ ). The similarity of the curves for  $x$  ranging from 0.5 to 1 indicated

(32) Christenson, H. K. *J. Phys.: Condens. Matter* **2001**, *13*, R95–R133.

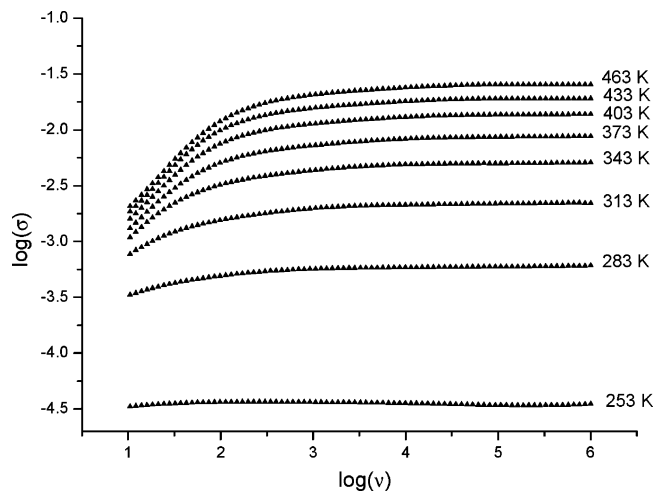


**Figure 6.** Conductivity vs frequency (log/log) at different temperatures for a silica-based ionogel ( $x = 0.5$ ).

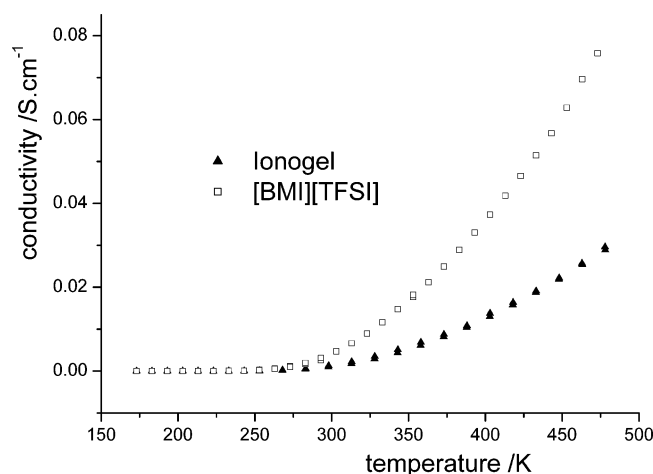


**Figure 7.** Conductivities vs temperature for the pristine ionic liquid ([BMI][TFSI]) and a silica-based ionogel ( $x = 0.5$ ).

close activation energies for the ionic conduction of the ionic liquid and the ionogels. The nonlinear plots led to roughly estimated activation energies within the range 0.2–0.4 eV between 250 and 500 K. It is worth noting that for  $x = 0.25$ , the curve was distinguished by an inflection point.

### Discussion

The rapid development of ionic liquid imidazolium salts as alternative solvents has given rise to numerous structural investigations. Thus, recent studies have evidenced that supramolecular interactions between dialkylimidazolium cations and anions was a common feature of this class of ionic liquids, which could be better described as supramolecular ions aggregates.<sup>33–35</sup> Some of these aggregates have been found even to be maintained in solution, at least in solvents of low dielectric constant.<sup>36</sup>

(33) Holbrey, J. D.; Reichert, W. M.; Nieuwenhuyzen, M.; Sheppard, O.; Hardacre, C.; Rogers, R. D. *Chem. Commun.* **2003**, 476.

(34) Hardacre, C.; Holbrey, J. D.; McMath, S. E. J.; Bowron, D. T.; Soper, A. K. *J. Chem. Phys.* **2003**, *118*, 273.

(35) Gozzo, F. C.; Santos, L. S.; Augusti, R.; Consorti, C. S.; Dupont, J.; Eberlin, M. N. *Chem.—Eur. J.* **2004**, *10*, 6187.

(36) Consorti, C. S.; Suarez, P. A. Z.; De Souza, R. F.; Burrow, R. A.; Farrar, D. H.; Lough, A. J.; Loh, W.; Da Silva, L. H. M.; Dupont, J. *J. Phys. Chem. B* **2005**, *109*, 4341.

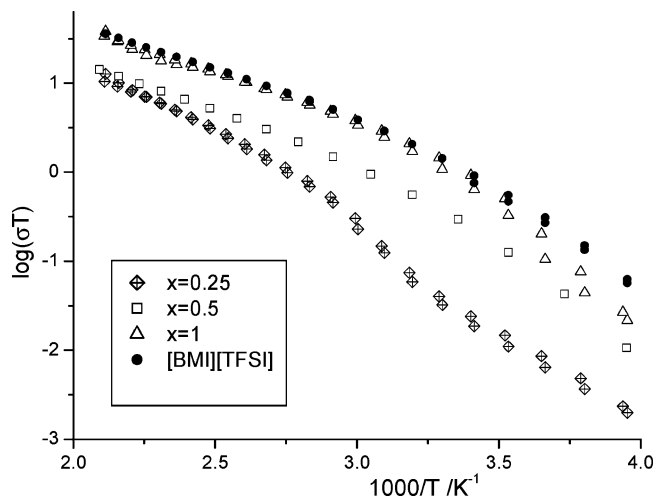


**Figure 8.** Conductivities (Arrhenius plots) of the ionic liquid ([BMI][TFSI]) and silica-based ionogels with different contents of ionic liquid.

To date there is no structural information about [BMI][TFSI]; however, the crystal structure of 1,3-dimethylimidazolium TFSI has recently been characterized by single-crystal X-ray diffraction.<sup>37</sup> The TFSI was shown to adopt the unexpected cis conformation constrained by bifurcated C(2)H···O bonding from the imidazolium cation to the anion, which resulted in fluorine sheets in a layered structure. Some related cation–anion interactions can be reasonably postulated in [BMI][TFSI].

DSC experiments disclosed the dramatic effect of confinement on the phase transitions of the ionic liquid within the ionogels. The disappearance of any clue of both cold crystallization and melting ( $T_m$ ) on increasing confinement (i.e., on decreasing the pore sizes by decreasing the ionic liquid content) is noticeable. Moreover, it is interesting to point out the case of  $x = 1.0$ , for which the melting was observed at a lower temperature ( $T'_m$ ) than for the pristine ionic liquid, whereas the cold-crystallization temperature  $T_{CC}$  was observed at higher value. Both temperatures were lower for methyl-modified silica.

Actually, according to simple mean field theory, the critical temperature of solid-to-liquid phase transition in confined liquids  $T'_c$  is expected to follow eq 1

$$T'_c = C \frac{z\epsilon}{k} \quad (1)$$

where  $z$  is the number of nearest neighbors,  $C$  a constant,  $\epsilon$  the interaction energy with the nearest neighbor, and  $k$  the Boltzmann constant.<sup>38</sup> Thus, confinement, which corresponds to a lowering of the average number of nearest neighbors, leads to a  $T'_m$  value lower than that of  $T_m$ . Further examination of the energy interface system lead to a Gibbs–Thomson-like eq 2

$$\frac{T'_c - T_c}{T_c} = -2 \frac{(\gamma_{p/s} - \gamma_{p/l})V_{mol}}{D\lambda_f} \quad (2)$$

(37) Holbrey, J. D.; Reichert, W. M.; Rogers, R. D. *Dalton Trans.* **2004**, 2267.

(38) Gelb, L. D.; Gubbins, K. E.; Radhakrishnan, R.; Sliwinski-Bartkowiak, M. *Rep. Prog. Phys.* **1999**, *62*, 1573.

where  $\gamma_{p/s}$  and  $\gamma_{p/l}$  are, respectively, the pore/solid and pore/liquid interface energies,  $V_{\text{mol}}$  the molar volume of the ionic liquid,  $\lambda_f$  the latent heat of melting, and  $D$  the pore diameter.  $T_c$  (here,  $T_m$ ) being lower than  $T_c$  (here,  $T_m$ ) is consistent with a higher pore/solid interface energy than pore/liquid interface energy, in accordance with a repulsive effect between the pore wall and the liquid.<sup>39</sup>

<sup>1</sup>H NMR spectroscopy indicates that the confined ionic liquid keeps some liquidlike molecular motions, even at a medium time scale (microsecond to millisecond). Chemical shift anisotropy and dipole–dipole interactions are fully averaged at a 0.4 kHz spinning rate, because raising spinning rate to 5 and 9 kHz does not bring about any decrease in fwhm, as expected when the resolution is limited by dipole–dipole interaction. Thus, the fwhm would be due to some dispersion in chemical shifts in relation to some dispersion in the nearest neighbors, as expected when going from the center of the pores to the walls. Moreover, <sup>1</sup>H NMR experiments at low temperatures disclose an effect of confinement on the glass transition, unlike DSC experiments. The striking fact is that the glass transition took place at a lower temperature in ionogels. It is worth underlining that  $T_g$  lowering was more marked in the methyl-modified sample.

Regarding crystallization temperatures, such behaviors are not surprising for confined fluids, as the number of molecules in the wall neighborhood is determining and the correlation length can grow to long range only in the pseudo-1D cylindrical-like pore axis direction. Nevertheless, the different behaviors of ionogels with and without methyl modification remains very interesting. The stability of TMOS/MTMS ionogels toward water, despite the repulsive wall/liquid effect, could be due to the presence of the hydrophobic methyl groups, which renders the wall/liquid interface interactions even less favorable to the neighborhood of water than that of the ionic liquid, and therefore erases the driving force of the replacement of the confined ionic liquid by water. Also unexpectedly, the overall effect of confinement, which

results in a lowering of dimensionality, seems to only weakly limit the molecular mobility.

The Arrhenius plots  $\log(\sigma T)$  vs  $(1 \times 10^3)/T$  (Figure 8) reflected lower activation energies at temperatures higher than 330 K. Such a break in the activation energy value around 330 K suggests either that two temperature-activated phenomena are involved in the overall charge transport, one of which is quenched by a strong confinement, or that a thermal phase transition occurs at 330 K (melting of a plastic crystal phase), modifying the molecular arrangement and/or the anisotropy.<sup>40–42</sup> If confirmed, such a transition would be one of the rare examples in confined systems. Additional investigations are under progress and should shed some light on these points in the near future.

## Conclusion

Ionogels containing non-water-soluble ionic liquids can be made stable toward water by modifying the silica matrix with hydrophobic organic groups as methyl groups; it is noteworthy that this modification does not change the thermal stability of ionogels. The data of DSC and <sup>1</sup>H NMR spectroscopy indicate that confinement gives the ionic liquid an intermediate behavior between liquid and solid. However, it is noteworthy that ionogels exhibit conduction performances similar to those of pristine ionic liquids despite the nanoscale level of confinement.

This feature, associated with excellent thermal stability and transparency, makes ionogels promising new solid-state electrolytes in such applications as dye-sensitized solar cells, fuel cells, and lithium batteries. Numerous applications derived from the solvent properties of ionic liquids could be addressed as well, such as catalysis, chromatography, and sensing.

CM060656C

(39) Evans, R.; Marini Bettolo Marconi, U. *J. Chem. Phys.* **1987**, *86*, 7138.

(40) MacFarlane, D.; Forsyth, M. *Adv. Mater.* **2001**, *13*, 957.

(41) Seeber, A. J.; Forsyth, M.; Forsyth, C. M.; Forsyth, S. A.; Annat, G.; MacFarlane, D. R. *Phys. Chem. Chem. Phys.* **2003**, *5*, 2692.

(42) Yoshio, M.; Mukai, T.; Ohno, H.; Kato, T. *J. Am. Chem. Soc.* **2004**, *126*, 994.